

Comparison between Curved-Mirrors and Flat-Mirrors of the Fixed Mirror Solar Concentrator Geometry

Ramon Pujol-Nadal¹, Víctor Martínez-Moll¹ and Andreu Moià-Pol¹

¹ University of Balearic Islands, Palma de Mallorca (Spain)

Abstract

There is a great unexploited potential for process heat applications in the medium temperature range (80-250°C). In this temperature range, the so-called tracking receiver, stationary reflector designs can reach high efficiencies (Gordon and International Solar Energy Society, 2001). Fixed Mirror Solar Concentrator (FMSC) design emerged in the seventies as an effort to reduce electricity production costs in solar thermal power plants (Russell et al., 1974). The reflector of the FMSC is composed by flat mirrors and remains static while the receiver is moving on a circle path. Replacing the flat mirrors by curved mirrors has the advantage of reaching higher concentrations, and this design has been called as Curved Slats Fixed Mirror Solar Concentrator (CSFMSC). In this communication an optical and thermal comparison between FMSC and CSFMSC is exposed based on recent investigations supported by ray-tracing tools. The local flux concentration, the incidence angle modifier (IAM) curves, and the IAM factorization are compared for both geometries. Finally the comparison between the annual thermal efficiency at 200°C for both geometries is exposed.

key-words: FMSC, CSFMSC, Fixed Mirror Solar Concentrator

1. Introduction

The FMSC consists of an arrangement of flat mirrors, with their respective central lines positioned along a circular path and oriented such that the rays reflected by the central points of the mirrors intersect at a point on the same base circle. It can be easily shown that for any incident angle, the reflected rays of the central lines of the mirrors will always intersect at a unique focus on the base circle and, therefore, it would be possible to track the sun simply by positioning the receiver at a certain angle over the circle path without moving the reflector, see Fig.1a. The FMSC design with curved mirrors has been called in the literature as CSFMSC (Balasubramanian and Sankarasubramanian, 1993) and consists of replacing the flat mirrors by curved mirrors in order to concentrate the sunlight in a single line (theoretical design) for normal incidence, see Fig. 1b.

For a recent study about a real implementation of a FMSC prototype see (Pujol-Nadal and Martínez-Moll, 2014b), and for a CSFMSC prototype see (Sallaberry et al., 2014). This technology has been patented by the Spanish company Tecnologia Solar Concentradora SL, www.tsc-concentra.com, (Martinez Moll et al., 2009b, Martinez Moll et al., 2009a)

In this communication a comparison between these two geometries has been conducted based on the optical and thermal analysis presented in previous studies (Pujol Nadal and Martínez Moll, 2012, Pujol Nadal and Martínez Moll, 2013, Pujol-Nadal et al., 2014, Pujol-Nadal and Martínez-Moll, 2014a).

The FMSC geometry is defined by three parameters, and the cases studied are the allowed combinations of the following values:

- Number of flat mirrors composing the reflector: $N=5, 7, \dots, 51$
- Focus to width ratio: $F/W=1.0, 1.25, \dots, 3.0$
- Intercept factor, defined as the fraction of the reflected radiation that is incident on the absorbing surface of the receiver (is related to the size of the receiver): $\gamma=0.92, 0.94, 0.96, 0.98$

On the other hand, the CSFMSC geometry is defined by three parameters too, and the cases studied are the allowed combinations of the following values:

- Number of parabolic mirrors composing the reflector: $N=1, 3, 5, 7$
- Focus to width ratio: $F/W=1.0, 1.25, \dots, 3.0$
- Aperture concentration ratio, is the ratio of the reflector aperture size to the receiver aperture size: $C_a=3, 4, 5, 18, 20, \dots, 30$

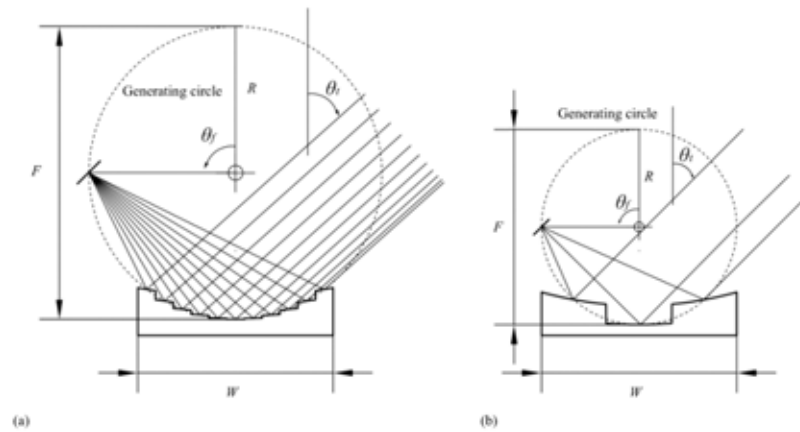


Fig. 1: (a) Optical principle of the FMSC. The receiver is moving in a circular path on the generating circle. The generating circle has a radius R , the focal length is $F=2R$, and the receiver is positioned by the θ_r angle. The position angle of the receiver is the double of the transversal incidence angle ($\theta_r=2\theta_i$). The reflector width is W . In this case $N=11$ mirrors and $F/W=1.5$. **(b) Optical principle of the CSFMSC.** The receiver has the same trajectory than the FMSC, in normal incidence all rays are focused on a single focus line. In this case $N=3$ mirrors and $F/W=1.0$.

2. Optical comparison

In this section an optical comparison between FMSC and CSFMSC geometries is presented highlighting on the radiation distribution on the absorber, the transverse and longitudinal IAM, and the IAM factorization results. All the calculation has been conducted using a ray-tracing program developed by the authors and exposed in (Pujol Nadal and Martínez Moll, 2012). For more details about the physical properties and the materials assumed in both geometries see the references (Pujol Nadal and Martínez Moll, 2012, Pujol Nadal and Martínez Moll, 2013).

2.1. Radiation distribution on the absorber

The local flux concentration ratio has been calculated for the following cases:

- FMSC: $N=13, F/W=1.75, \gamma=0.98$
- CSFMSC: $N=1, F/W=1.75, C_a=8$

These cases are selected because are some of the most efficient designs, as it is shown in the Section 3. In the Fig. 2 the local flux concentration ratio for the selected geometries is shown. Comparing both results it can be seen that the Curved-Mirrors achieve a local flux concentration of 20 in front of 9 of the other case. About the optical efficiency, it can be observed how the CSFMSC reach higher efficiencies when the transversal angle increases, while in the Flat-Mirrors case, the optical efficiency drops when the transversal incidence angle increases. This is due to the rays that are intercepted on the steps and that therefore do not reach the receiver.

It can be observed that the local flux concentration of the CSFMSC case is asymmetric when the transversal incidence angle increases (part of the energy is lost on one side of the receiver). Meanwhile in the Flat-Mirrors case the flux concentration on the receiver is quite symmetric and fewer losses are detected in the tails of the radiation distribution.

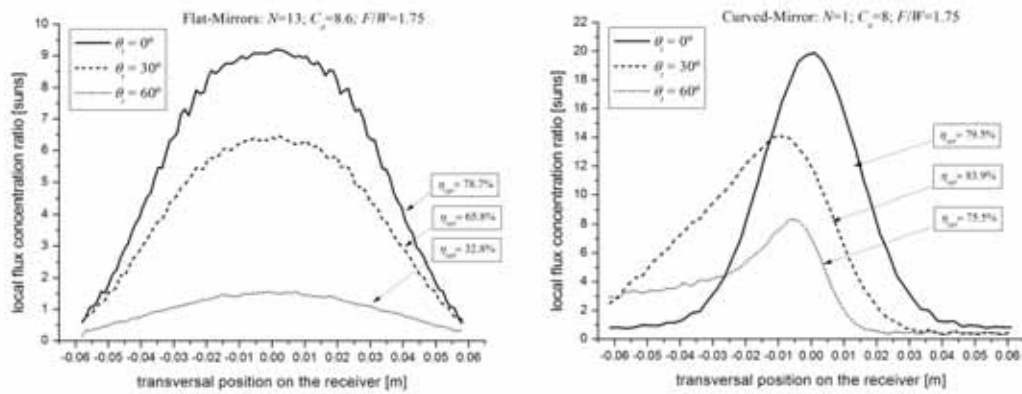


Fig. 2: Local distribution of the radiation on the receiver for two selected cases.

2.2 Optical efficiency at normal incidence

The optical efficiency at normal incidence has been calculated and exposed in the Fig. 3 for three selected cases of both geometries. It can be observed that the optical efficiency for the FMSC geometry is independent of the number of mirrors, meanwhile the optical efficiency for CSFMSC designs decreases when the aperture concentration increases. This is due to the fact that receiver is too small to intercept all the rays reflected by the mirror. It can be noted that for concentration factors lower than 14 the CSFMSC reaches higher optical efficiencies than the FMSC designs, because with the parabolic design there are no ray interferences with the reflector steps.

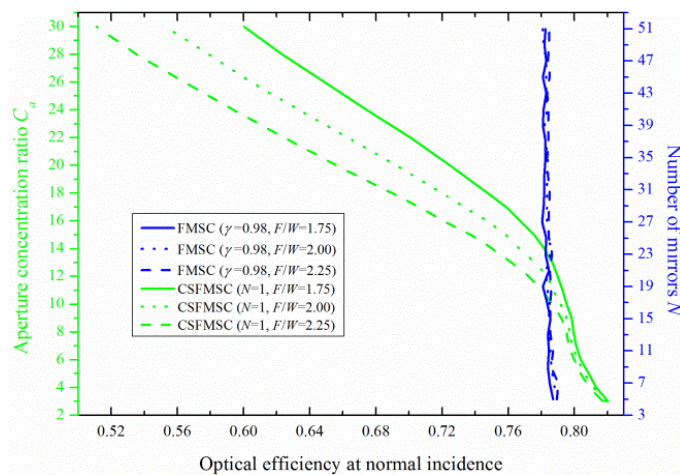


Fig. 3: Optical efficiency at normal incidence as a function of the number of mirrors for the FMSC, and as a function of the aperture concentration for the CSFMSC.

2.3 Transverse and longitudinal IAM

The transverse and longitudinal IAM for selected cases of Curved-Mirrors and Flat-Mirrors designs are shown in Fig. 4. The transverse IAM is shown in Fig. 4a, and the longitudinal in Fig. 4b. For the Flat-Mirrors designs it can be seen that by increasing the number of mirrors, the transversal IAM decreases, which is due to the fact that increasing N increases the number of steps of the concentrator and therefore the probability that the rays are intercepted on the steps and do not reach the receiver. For the CSFMSC, the results show

that increasing the concentration causes the transversal IAM to decrease, which is due to the fact that increasing the aperture concentration C_a decreases the size of the receiver, and therefore a portion of the reflected radiation does not reach the receiver. Note also that in some cases the curve takes a value that is greater than 1; this is because some of the radiation goes directly to the receiver without being reflected by the mirror and, thus, more energy can be captured than reaches the reflector aperture.

About the longitudinal IAM and for the Flat-Mirrors designs, it can be seen that increasing the number of mirrors also produces a reduction in the longitudinal IAM values, see Fig. 4b. This is mainly because when N decreases the size of the receiver increases and a large receiver captures more energy that comes directly from the sun without being reflected by the mirrors. For the CSFMSC designs a similar behaviour can be seen, an increasing of C_a produces a reduction in the longitudinal IAM values. This is because an increase in C_a causes the size of the receiver to decrease, and a smaller receiver captures less energy.

It can also be noted that the CSFMSC is more sensitive to variations of C_a than the FMSC to variations in N .

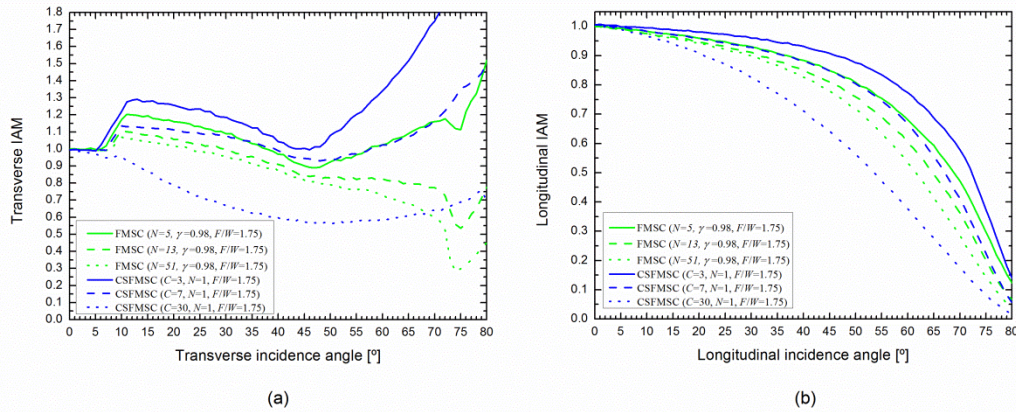


Fig. 4: (a) Transverse IAM curves and (b) Longitudinal IAM curves

2.4 IAM factorization

For the FMSC and CSFMSC theoretical designs in (Pujol Nadal and Martínez Moll, 2012, Pujol Nadal and Martínez Moll, 2013) it was shown that the IAM can be factorized in a similar way to the CPC collectors by the product of the transverse and longitudinal IAM, $K(\theta_T, \theta_L) \approx K(\theta_T, 0)K(0, \theta_L)f(\theta_T, \theta_L)$, where $f(\theta_T, \theta_L)$ is a function that takes into account the longitudinal end losses. On the other hand the real IAM value $K(\theta_T, \theta_L)$ has been calculated with the ray-tracing program in order to compare with the approximation via factorization. The Root Mean Square Error (RMSE) has been determined for each design using the following equation:

$$\text{RMSE} = \left[\frac{1}{N_p} \sum \Delta K^2 \right]^{1/2} \quad (\text{eq. 1})$$

where ΔK is the difference between IAM factorization and the value obtained by ray-tracing

$$\Delta K = [K(\theta_T, 0)K(0, \theta_L)f(\theta_T, \theta_L) - K(\theta_T, \theta_L)] \cos(\theta_i) \quad (\text{eq. 2})$$

In eq. (2) the θ_i angle is the incident angle, and the function $f(\theta_T, \theta_L)$ that takes into account the longitudinal end losses is:

$$f(\theta, \theta_i) = \begin{cases} \frac{L - [R + R \cos(2\theta)] \tan(\theta_i)}{L - 2R \tan(\theta_i)} & \theta_i < \theta_{i,\text{lim}} \text{ and } \theta_i < 75 \\ \frac{L - [R + R \cos(2\theta_{i,\text{lim}})] \tan(\theta_i)}{L - 2R \tan(\theta_i)} & \theta_i \geq \theta_{i,\text{lim}} \text{ and } \theta_i < 75 \\ 1 & \theta_i \geq 75 \end{cases} \quad (\text{eq. 3})$$

where L is the length of the concentrator in the longitudinal dimension ($L=10$ m) and $\theta_{t,LIM}$ is the transversal incidence angle when the intersection between the receiver and the reflector occurs. For more details about the Eq.(3) see the references cited above.

In Figs. 5a-b the RMSE has been calculated for both geometries. It can be observe that the RMSE values are similar for both designs, although Curved-Mirrors designs presents lower values when $C_a=7-9$.

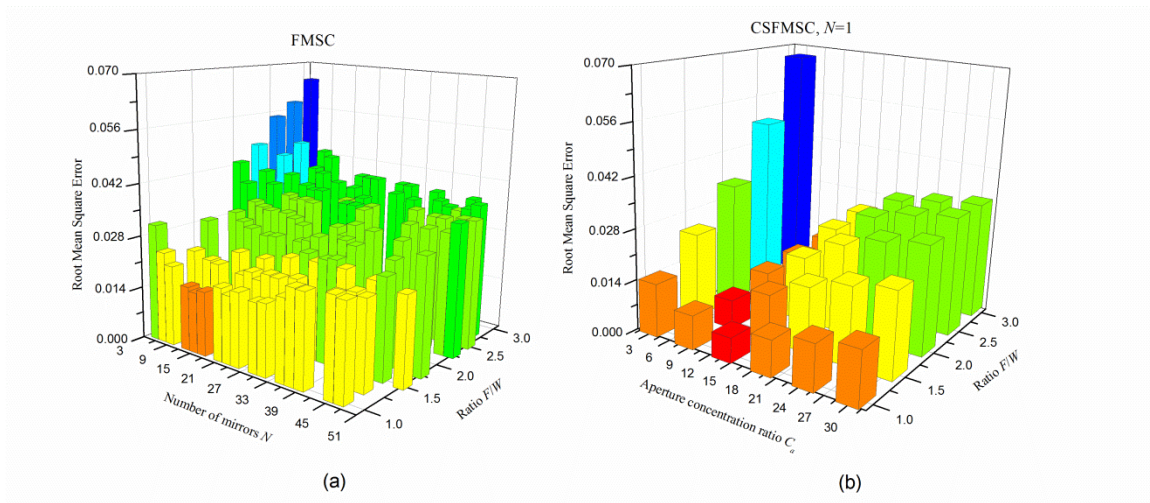


Fig. 5: RMSE in the calculation of the energy collected from direct radiation if $K \sim K(\theta_n, \theta)K(0, \theta)f(\theta_n, \theta)$ is used instead of value obtained by ray-tracing program $K(\theta_n, \theta)$.

3. Thermal comparison

The annual thermal efficiency at an average working temperature of 200°C has been calculated. The locations considered have been: Cairo, Palma de Mallorca and Munich. For more details about the procedure see (Pujol-Nadal et al., 2014, Pujol-Nadal and Martínez-Moll, 2014a). The average thermal efficiency in NS and EW orientation for the three locations considered is exposed in Fig. 6. It can be observed that the CSFMSC design reaches higher efficiencies than the Flat-Mirrors design, but is quite sensitive to the aperture concentration ratio. The best design is composed by one parabolic mirror, $F/W=2.0$, and $C_a=7-8$.

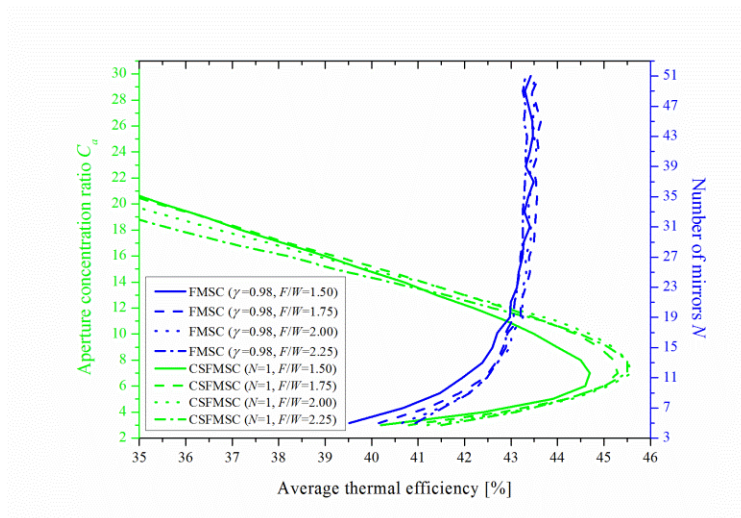


Fig. 6: Average values of the thermal efficiency in NS and EW orientation for the three locations considered (Cairo, Palma de Mallorca and Munich).

4. Conclusions

Fixed-Mirror designs have a great potential for solar heating in the medium temperature range. These geometries emerged respectively in the seventies and the nineties. In this communication a comparison between them is presented for the first time based on recent studies supported by 3D ray-tracing simulations.

The CSFMSC designs present better optical and thermal behavior compared to FMSC designs for the selected design parameters. The CSFMSC composed by only one parabolic mirror has a simpler design than the stepped geometry of the FMSC, and has a higher annual energy yield. Hence it can be concluded that a Fixed-Mirror solar concentrator composed by one parabolic mirror is the best design that can be constructed of the geometries analyzed.

5. References

Balasubramanian, V., Sankarasubramanian, G., 1993. Stretched tape design of fixed mirror solar concentrator with curved mirror elements. *Solar Energy* 51, 109-119; doi: 10.1016/0038-092X(93)90073-W.

Gordon, J.M., International Solar Energy Society, 2001. *Solar Energy :The State of the Art : ISES Position Papers*. James & James, London.

Martinez Moll, V., Pujol Nadal, R., Montesino Semper, J., Moia Pol, A., Paz Bernales, H., Trobat Obrador, G., 2009a. Reflector-concentrator unit for solar collector unit, comprises sandwich structure with top sheet which has associated outer surface to reflect incident rays and concentrating rays in linear focus. Spanish Patent. ES2322837-A1. ES003463 28 Dec 2007.

Martinez Moll, V., Pujol Nadal, R., Paz Bernales, H., Martinez Verdu, D., Moia Pol, A., Riba Romeva, C., Schweiger, H., 2009b. Solar energy concentrator and collector device for collecting thermal energy from solar rays, has tracking mechanism that supports and moves mobile structure of mobile receiver on appropriate stationary reflector and concentrator. Spanish Patent. ES2326353-B1. ES003464 28 Dec 2007.

Pujol Nadal, R., Martínez Moll, V., 2013. Optical analysis of a curved-slats fixed-mirror solar concentrator by a forward ray-tracing procedure. *Applied Optics* 52, 7389-7398; doi: 10.1364/AO.52.007389.

Pujol Nadal, R., Martínez Moll, V., 2012. Optical analysis of the fixed mirror solar concentrator by forward ray-tracing procedure. *ASME Journal of Solar Energy Engineering* 134, 031009-1-14; doi: 10.1115/1.4006575.

Pujol-Nadal, R., Martínez-Moll, V., Moia-Pol, A., 2014. Parametric Analysis of the Fixed Mirror Solar Concentrator for Medium Temperature Applications. *ASME Journal of Solar Energy Engineering* 136, 011011-1-7; doi: 10.1115/1.4026098.

Pujol-Nadal, R., Martínez-Moll, V., 2014a. Parametric analysis of the curved slats fixed mirror solar concentrator for medium temperature applications. *Energy Conversion and Management* 78, 676-683; doi: j.enconman.2013.11.032.

Pujol-Nadal, R., Martínez-Moll, V., 2014b. Optical characterization of a fixed mirror solar concentrator prototype by the ray-tracing procedure. *Journal of Renewable and Sustainable Energy* 6, 043105 (2014); doi: 10.1063/1.4890219.

Russell, J.L., DePlomb, E.P., Bansal, R.K., 1974. *Principles Of The Fixed Mirror Solar Concentrator*, 2nd ed., General Atomic Co., San Diego, CA, Report No. GA-A12903.

Sallaberry, F., Pujol-Nadal, R., Martínez-Moll, V., Torres, J., 2014. Optical and thermal characterization procedure for a variable geometry concentrator: A standard approach. *Renewable Energy* 68, 842-852; doi: 10.1016/j.renene.2014.02.040.